Keiji Ueno
Tomohiro Shida, Shuuto Horii
Saitama University, 255 Shimo-Okubo, Sakura-ku, Saitama, Japan

kei@chem.saitama-u.ac.jp

Relaxation of Fermi-level Pinning in 2H-$MoSe_2$ FET by Inserting 1T-phase Buffer Layers into Source/Drain Contacts

A semiconducting transition metal dichalcogenide (TMDC) is gathering much attention as a post-silicon source material for field-effect transistor (FET) due to its attractive scaling character; monolayer TMDC having a sub-nm thickness can act as the current channel of FET. In most TMDC FET, however, Fermi-level pinning (FLP) occurs at source/drain electrode contacts, which often restricts the operation characteristics and performances of TMDC FET. For example, in the case of MoS_2 FET, Fermi levels of a various metal electrodes are strongly pinned just below the conduction band minimum of MoS_2. Then, only the n-type FET operation has been observed for most metal electrodes. In the case of $MoSe_2$ FET, we have revealed the existence of FLP in un-doped n-type FETs and arsenic-doped p-type FETs for Pt, Au and Ti/Au electrodes by measuring Schottky barrier heights at their electrode contacts. However, if FLP is relaxed, the Schottky barrier height can be reduced by adjusting the work function of the electrode material, and the FET performance will be improved.

Here, we report the relaxation of FLP in 2H-$MoSe_2$ FETs by inserting 1T-phase buffer layers into source/drain electrode contacts. In the case of $MoSe_2$, similar to MoS_2, the semiconducting 2H phase (Fig. 1(a)) is most stable and the metallic 1T phase (Fig. 1(b)) is unstable. Recently, it was reported that exposure to Ar/H_2 mixture-gas plasma changed the surface of 2H-MoS_2 to the 1T phase [1]. Thus, we adopted this technique to fabricate the 1T-phase buffer layer in 2H-$MoSe_2$ FET, and investigated the FLP relaxation.

Bulk single-crystals of un-doped 2H-$MoSe_2$ were grown by the chemical vapor transport method without using a halogen transport agent [2]. FETs were fabricated on SiO_2(285 nm)/p^{++}-Si substrates by the mechanical exfoliation/transfer method using an adhesive tape. Source/drain electrodes (Pt, Au or Ti/Au) were deposited via photolithography, sputtering and lift-off processes. When the insertion of the 1T-$MoSe_2$ buffer layer was examined, the transferred clean 2H-$MoSe_2$ flakes were first exposed to the Ar/H_2 (95:5 volume ratio) mixture-gas plasma (20 sccm, 200 Pa, 160 W) for 1 h. Next, source/drain electrodes were deposited onto the 1T-$MoSe_2$ buffer layer. Finally, a focused laser beam (532 nm) was linearly scanned just between the source/drain electrodes to remove only the 1T-$MoSe_2$ buffer layer and fabricate a narrow 2H-$MoSe_2$ FET channel. These processes are schematically summarized in Fig. 2.

Figure 3 shows transfer characteristics of two 2H-$MoSe_2$ FETs with Au source/drain electrodes fabricated before and after the Ar/H_2 plasma irradiation. Before the irradiation 2H-$MoSe_2$ FET showed usual n-type operation, but the plasma irradiation apparently changed the $MoSe_2$ channel to metallic with higher carrier concentration. Figure 4(a) shows transfer characteristics of three 2H-$MoSe_2$ FETs with source/drain electrodes of Pt, Au and Ti/Au. Although work functions of Pt (5.65 eV), Au (5.1 eV) and Ti (4.33 eV) are largely different, transfer curves of three FETs are not so different, which indicates the existence of strong FLP at source/drain electrode junctions. After the insertion of 1T-$MoSe_2$ buffer layers, however, transfer curves of three FETs having different metal electrodes show far larger differences, as shown in Fig. 4(b). Due to the relaxation of FLP, the Schottky barrier height for the electron injection into the $MoSe_2$ conduction band from the Pt electrode, which has the largest work function, becomes far higher than that of Ti, which results in the smallest and the largest ON-current of FET for Pt and Ti/Au electrodes, respectively.

References

[1] C. H. Sharma, A. P. Surendran, A. Varghese and M. Thalakulam, Sci. Rep. **8** (2018) 12463.
[2] K. Ueno, J. Phys. Soc. Jpn. **84** (2015) 121015.

Figures

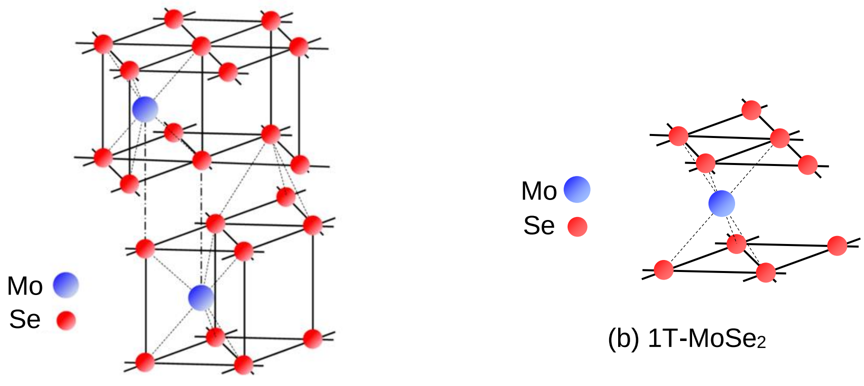

Figure 1: Crystal structures of (a) 2H-$MoSe_2$ and (b) 1T-$MoSe_2$.

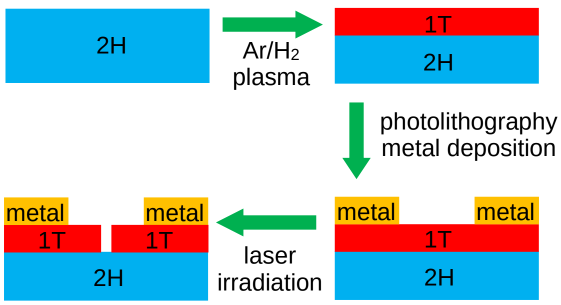

Figure 2: Fabrication of 2H-$MoSe_2$ FET with 1T-$MoSe_2$ buffer layers.

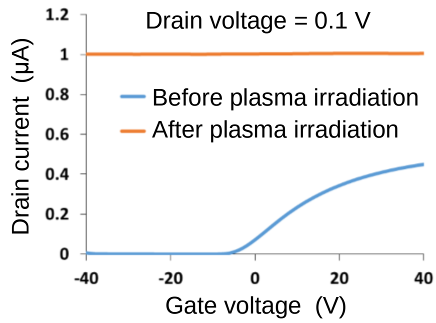

Figure 3: Transfer characteristics of 2H-$MoSe_2$ FETs before and after plasma irradiation (Au electrodes).

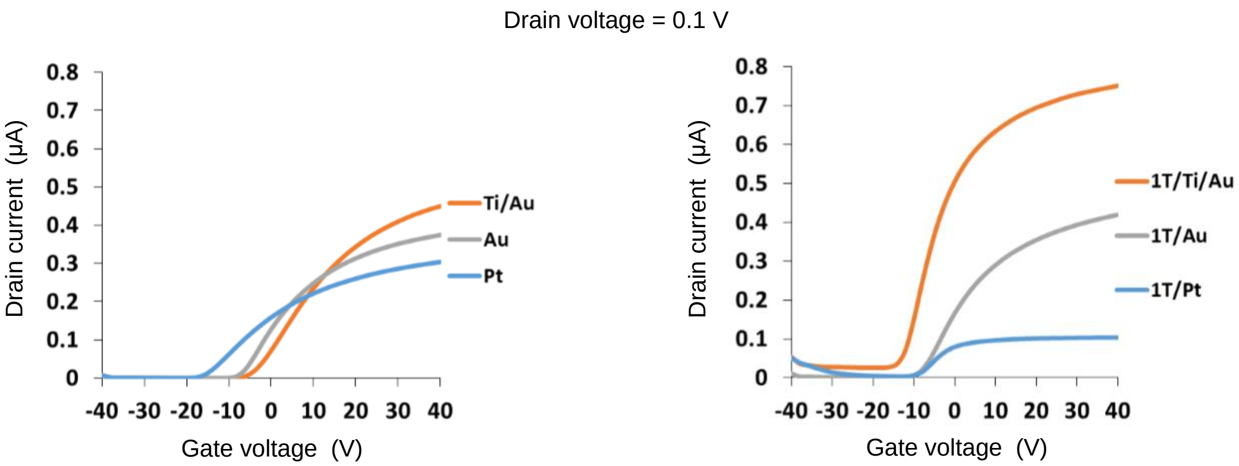

(a) 2H-$MoSe_2$ FETs

(b) 2H-$MoSe_2$ FETs with 1T-$MoSe_2$ buffer layers

Figure 4: Transfer characteristics of 2H-$MoSe_2$ FETs; (a) without and (b) with 1T-$MoSe_2$ buffer layers.